

BRIEF COMMUNICATION

**STRATEGIES FOR CELL SHAPE CONTROL IN TIP-GROWING CELLS<sup>1</sup>**

OTGER CAMPÀS<sup>2,3,5</sup>, ENRIQUE ROJAS<sup>3,4</sup>, JACQUES DUMAIS<sup>3,6</sup>, AND L. MAHADEVAN<sup>2–5</sup>

<sup>2</sup>School of Engineering and Applied Sciences, Harvard University, Cambridge, Massachusetts 02138 USA;

<sup>3</sup>Department of Organismic and Evolutionary Biology, Harvard University, Cambridge, Massachusetts 02138 USA,

<sup>4</sup>Department of Physics, Harvard University, Cambridge, Massachusetts 02138 USA

- *Premise of the study:* Despite the large diversity in biological cell morphology, the processes that specify and control cell shape are not yet fully understood. Here we study the shape of tip-growing, walled cells, which have evolved a polar mode of cell morphogenesis leading to characteristic filamentous cell morphologies that extend only apically.
- *Methods:* We identified the relevant parameters for the control of cell shape and derived scaling laws based on mass conservation and force balance that connect these parameters to the resulting geometrical phenotypes. These laws provide quantitative testable relations linking morphological phenotypes to the biophysical processes involved in establishing and modulating cell shape in tip-growing, walled cells.
- *Key results and conclusions:* By comparing our theoretical results to the observed morphological variation within and across species, we found that tip-growing cells from plant and fungal species share a common strategy to shape the cell, whereas oomycete species have evolved a different mechanism.

**Key words:** cell wall; morphogenesis; morphological variation; tip-growth; walled cells.

Unicellular organisms, as well as the different cell types in multicellular organisms display a remarkable variation in size and shape (Mathur, 2004; Gilbert, 2006; Young, 2006; Lecuit and Lenne, 2007). Despite the significance of cell morphology for cellular function, neither the mechanisms that establish and maintain cell shape in a given species nor the mechanisms for shape variation across species are entirely understood. Most cellular morphogenesis studies have focused on molecular aspects of cellular structures (e.g., the cytoskeleton, transport mechanisms), as well as the intracellular signaling events that control these molecular interactions (Macara, 2004; Mathur, 2004; Cabeen and Jacobs-Wagner, 2005; Krichevsky et al., 2007). While knowledge of the molecular components and their spatiotemporal interactions is certainly critical in building toward a mechanistic understanding of cellular morphogenesis, at larger (mesoscopic) scales, these processes must eventually be integrated with the basic conservation laws of physics, and in particular mass conservation and force balance. This is a difficult challenge in animal cells with a fluid bilayer envelope that is actively shaped by the underlying dynamic cytoskeletal cortex (Gilbert, 2006; Farhadifar et al., 2007; Lecuit and Lenne, 2007).

However, most prokaryotes and many eukaryotes such as water molds, fungal cells, and plants are composed of walled cells and are thus particularly well suited to address these questions

because the shape of the cell is well defined by the location of a relatively stiff cell wall. As a consequence, these organisms can only explore new environments through the process of cell extension or growth. This potential handicap has been overcome by walled cells of many different species, which have converged on a common functional solution known as tip growth—a polar mode of cell morphogenesis leading to characteristic filamentous cell morphologies that extend only apically (Hepler et al., 2001; Harold, 2005; Cole and Fowler, 2006; Krichevsky et al., 2007). This filamentous growth mode allows walled cells to explore vast regions of space maintaining their metabolic rates, as the surface-to-volume ratio of the cell remains unchanged in a tubular geometry. While the geometry of the cell away from the growing region is that of a simple cylinder, in the apical growing region the shape of the cell is more complex and differs across species (interspecific variation) and even within a given species (intraspecific variation) (Fig. 1). The molecular and cellular mechanisms controlling morphogenesis in phylogenetically distant species are distinct (Geitmann and Emons, 2000; Heath and Geitmann, 2000), but in all cases, they share some common features at the level of cell wall remodeling during tip growth (Harold, 2005).

Here we focus on the particular case of tip-growing cells and study the role of cell wall assembly and expansion on cell shape. We first describe the physics of cell wall expansion and derive scaling laws that relate the geometry of the cell to the physical parameters relevant in shaping the cell at the mesoscopic scale. By comparing the patterns of morphological variation observed in tip-growing cells from different species to the theoretical results, we identified the physically relevant parameters that different species regulate to modify and control cell shape. Although plant and fungal species differ in the molecular and cellular mechanisms of morphogenesis (Geitmann and Emons, 2000; Heath and Geitmann, 2000), they share a common strategy to assemble the cell wall, leading to a common pattern of morphological variation. In contrast, we find that oomycete species (water molds) control cell wall

<sup>1</sup>Manuscript received 25 February 2012; revision accepted 31 July 2012.

The authors thank the Harvard-Kavli Institute for Nano-bio Science and Technology, the Wyss Institute for Biologically Inspired Engineering, the Human Frontier Science Program, and the MacArthur Foundation for partial financial support. O.C. and E.R. contributed equally to this work.

<sup>5</sup>Authors for correspondence (e-mail: lm@seas.harvard.edu, ocampas@seas.harvard.edu)

<sup>6</sup>Present address: Facultad de Ingeniería y Ciencias, Universidad Adolfo Ibáñez, Avda. Padre Hurtado 750, Viña del Mar, Chile

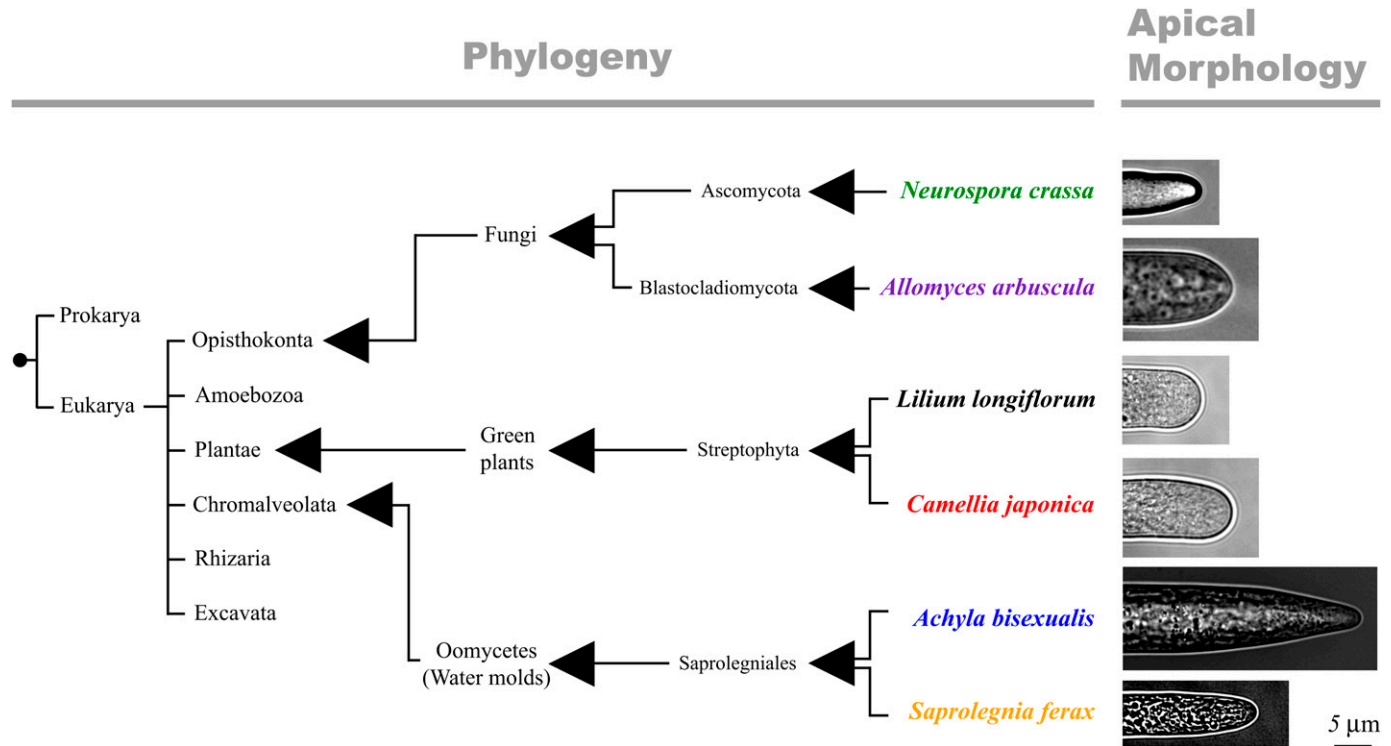


Fig. 1. Phylogenetic relations and apical cell shapes in tip-growing cells of several species. Phylogenetic relations of the species used in our study, which span three major eukaryotic groups, Plants, fungi and water molds (for a detailed phylogeny of eukaryotes, see Simpson and Roger, [2004]). Triangles in the phylogeny indicate that, although only one or few species or subgroups of the parent group are shown, the group contains more species or subgroups. We considered two species from each of the eukaryotic groups studied. Pollen tubes of *Camellia japonica* and *Lilium longiflorum* were chosen to represent the plant world. Hyphae of the model organism *Neurospora crassa* and of *Allomyces arbuscula* were chosen as examples of tip growth in fungal species. To represent oomycetes (water molds), we chose the species *Achlya bisexualis* and *Saprolegnia ferax*. The characteristic morphologies of the growing apical regions of tip-growing cells from each of these species are shown.

expansion using a different strategy than plant and fungal cells, leading to a very distinct pattern of morphological variation.

## MATERIALS AND METHODS

**Sample preparation**—Lily pollen was obtained from the flowers of *Lilium longiflorum* plants as their anthers dehiscid. Camellia pollen was obtained from the flowers of *Camellia japonica* plants (courtesy of Anja Geitmann and the Montreal Botanical Garden). Pollen was desiccated for 24 h and then freeze-dried at  $-20^{\circ}\text{C}$  for storage. Lily pollen grains were germinated in a growth medium based on one used by (Holdaway-Clarke et al., 1997), consisting of 15 mmol/L MES, 1.6 mmol/L  $\text{H}_3\text{BO}_3$ , 0.1 mmol/L KCl, 7.5% sucrose [m/v], adjusted to pH 5.3 with 0.1 mmol/L KOH. Camellia pollen grains were germinated in a medium consisting of 1.6 mmol/L  $\text{H}_3\text{BO}_3$ , 2.5 mmol/L  $\text{Ca}(\text{NO}_3)_2 \cdot \text{H}_2\text{O}$ , 1 mmol/L  $\text{KNO}_3$ , 0.8 mmol/L  $\text{MgSO}_4 \cdot 7\text{H}_2\text{O}$ , and 8% sucrose (w/v). Pollen grains were germinated on a thin layer (<1 mm) of 1% low-melting-point agarose on the bottom of a custom-made chamber, consisting of a polymer gasket affixed to a cover glass. While the agarose was still in a molten state, it was rinsed with a suspension of pollen grains in liquid growth medium. Pollen grains that remained on the surface of the agarose were fixed into place as the gel solidified. Cells that emerged from grains that were affixed to the agarose surface in this manner were likely to grow along the gel–liquid interface and were thus ideal for imaging. The slide chambers were then reimmersed in liquid medium and sealed on top with a cover glass.

*Achlya bisexualis*, *Saprolegnia ferax*, and *Allomyces arbuscula* cultures (all obtained from Carolina Biological Supply, Burlington, North Carolina, USA) were propagated on solid yeast-malt medium (0.3% yeast extract, 0.3% malt extract, 0.5% peptone, 1% dextrose, and 1% agarose [w/v] in water). For the imaging of *Achlya* and *Saprolegnia*, polymer slide chambers were prepared, similar to those for pollen, with 1% low-melting-point agarose yeast-malt

medium. The slide chambers were inoculated with the propagation culture after the medium had solidified, and then sealed with a cover glass. The slide chambers were imaged after 24 h. For imaging of *Allomyces*, cultures were propagated in special cover-glass-bottomed Petri dishes (MatTek). The bottom of the dishes are covered in a layer ( $\approx 0.2\text{mm}$ ) of solid growth medium (1% agarose), and one edge of the substrate is inoculated. The hyphae tend to grow in the thin layer of liquid between the cover glass and the agarose at the bottom of the dish. Growing hyphae were imaged 5–6 d after inoculation.

*Neurospora crassa* cultures (courtesy of Anne Pringle, Harvard University) were propagated on a solid growth medium based on one developed by Westergaard and Mitchell (1947) consisting of 0.1%  $\text{KNO}_3$ , 0.1%  $\text{KH}_2\text{PO}_4$ , 0.05%  $\text{MgSO}_4$ , 0.01%  $\text{CaCl}_2$ , 0.01%  $\text{NaCl}$ , 2% sucrose (w/v), 5  $\mu\text{g}$  biotin/L water and trace elements in the concentrations given in (Beadle, 1945). For imaging, slide chambers were prepared in the same manner as for *Achlya* and *Saprolegnia*.

**Imaging and image analysis**—All cells were imaged through a  $60\times$  water immersion lens and a  $1.6\times$  projection lens, for a total magnification of  $96\times$ , on an inverted microscope (Olympus, Center Valley, Pennsylvania, USA). Time-lapse images were recorded with a 14-bit cooled CCD camera (PCO 1600). IPLab (Scanalytics, Rockville, Maryland, USA) was used for image acquisition. Cells were imaged at time intervals of 2–4 s for pollen tubes, 3–5 s for oomycete hyphae, 10–20 s for *Allomyces* hyphae, and 2–4 s for *Neurospora* hyphae.

Images were analyzed using ImageJ and Matlab (Mathworks, Natick, Massachusetts, USA). Time-lapse images were first filtered with a 1 pixel radius median filter in ImageJ. The image sequences were then loaded into Matlab, where the rest of the analysis was performed with custom-written routines. The bright field images were filtered with a Canny edge detector, which returns a binary, 1 pixel-wide outline of the cell. This outline was manually identified in the first two images of the sequence. The program then automatically tracked the movement of the cell outline over the entire image sequence. The outlines were then interpolated to find the coordinates of the fiducial markers,  $P_i$ , which

were spaced equidistantly ( $ds$ ) along the outlines. The vectors normal to the lines connecting the fiducial points,  $N_i$ , were found, and then the meridional curvature of the outlines was calculated from the expression  $\kappa_i = \frac{\phi_{i+1} - \phi_i}{ds}$ , where  $\phi_i$  is the angle of  $N_i$  with respect to an arbitrary axis. The curvature profile was averaged over the image sequence. The location of the pole was taken to be the point around which the curvature profile had the highest reflection symmetry. The polar radius was calculated by  $R_A = \frac{1}{\kappa_{\text{pole}}}$ . The radius of the cell was found by integrating  $\phi$  along the meridian,  $R = \int_{\text{pole}}^S \cos(\phi) ds$ , where  $S$  is an arc length on the cylindrical portion of the cell.

## RESULTS

**Physical aspects of cell shape**—Walled cells are externally bounded by a thin polymeric layer that surrounds the cell and defines its shape. Since the walls are fairly stiff, cell shape is thus dictated by the processes of cell wall assembly and expansion. Tip-growing cells, our focus here, have been extensively studied in several species from many different perspectives. While many studies focus on the molecular mechanisms of tip growth (Heath and Geitmann, 2000; Hepler et al., 2001; Cole and Fowler, 2006; Krichevsky et al., 2007; Steinberg, 2007; Lew, 2011), several groups have also studied its biophysical aspects in various organisms (Green et al., 1970; Harold, 2005; Geitmann and Ortega, 2009). Experimentally, the focus has been on understanding the molecular and cellular dynamics of vesicular transport, cell wall expansion, and the concomitant geometry changes (Castle, 1958; Hejnowicz et al., 1977; Ortega, 1990; Money and Harold, 1992; Shaw et al., 2000; von Dassow et al., 2001; Bolduc et al., 2006; Zerzour et al., 2009), while theoretical studies have usually either focused on the geometry (Pelce and Pocheau, 1992) and the mechanics of cell wall expansion (Lockhart, 1965; Veytsman and Cosgrove, 1998; Goriely and Tabor, 2003; Wei and Lintilhac, 2003; Dumais et al., 2006; Kroeger et al., 2008; Fayant et al., 2010) or on the kinetics of assembly of new cell wall material (Gierz and Bartnicki-Garcia, 2001; Tindemans et al., 2006), and only rarely on both (Campas and Mahadevan, 2009; Rojas et al., 2011).

Tip-growing cells maintain a high osmotic pressure difference between the inside and outside of the cell. This high internal pressure (turgor), which is mechanically sustained by the cell wall, acts as the driving force for cell wall expansion during cell growth. The cell wall of tip-growing cells expands only at the apical region of the cell, and it does so irreversibly (Schopfer, 2006; Krichevsky et al., 2007): if the difference in internal and external pressures is reversed, the cell wall keeps its shape (shrinking only by about 5%). Thus, while the growing apical cell wall is likely to behave elastically at short time scales compared to growth, on the typical time scale of cell growth, it flows, and is not a simple elastic material. Indeed, studies going back to the pioneering work of Lockhart (1965) have shown that the wall is viscoelastic (or viscoplastic) behavior and implies that it deforms irreversibly during material addition and expansion.

Therefore, the turgor induced, irreversible expansion of the cell wall in the apical region of a tip-growing cell can be minimally described as the extension a thin nonhomogenous viscous shell with lowest viscosity  $\mu_0$  at the apex due to the higher concentration of cell wall loosening enzymes in this region (Campas and Mahadevan, 2009). Far away from the growing region, the tubular cell shape is likely fixed by rigidifying the cell wall, in accordance with experimental data showing that the cell wall away from the apical growing region behaves as an elastic material (Schopfer, 2006). The transition from a fluid-like

flowing cell wall at the apex to a stiff elastic cell wall away from the apex is likely to occur through a gelation transition and is consistent with the observed increase of cross-links between cell wall polymers away from the growing apical region in pollen tubes (Bosch and Hepler, 2005). At a mesoscopic level then, cell wall morphogenesis is constrained by the addition of new cell wall material, as well as the balance of forces in the cell wall.

At a scaling level, we first recapitulate the results of (Campas and Mahadevan, 2009). The steady apical expansion of the cell requires a constant secretion of new cell wall material at the apex (with rate  $\gamma_A$  per unit surface), which is sustained by a material flux  $J_\infty$  transported intracellularly along cytoskeletal structures from the synthesis machinery (Golgi apparatus) (Harold, 2005; Krichevsky et al., 2007). Mass conservation dictates that  $J_\infty = \pi a^2 \gamma_A$ , defining the size  $a$  of the region over which secretion occurs apically (Fig. 2A). Comparing the local expansion rate  $PR_A/\mu_A$  induced by a turgor pressure  $P$  at the tip of radius  $R_A$  (Fig. 2A), to the velocity  $\gamma_A/\rho_w$  at which a cell wall with density  $\rho_w$  is assembled apically, yields the apical radius of curvature

$$R_A \sim \frac{\mu_A \gamma_A}{P \rho_w} \quad (1)$$

Similarly, balancing the cell wall areal expansion rate,  $P/\mu_A R^2$ , with the areal rate of cell wall addition,  $J_\infty/R\rho_w$ , yields the cell radius

$$R \sim \left( \frac{J_\infty \mu_A}{\rho_w P} \right)^{1/3}, \quad (2)$$

as a function of the relevant physical magnitudes in the problem. Numerical integration of the steady-state equations of cell wall expansion in tip-growing cells (Campas and Mahadevan, 2009), is consistent with the scaling laws derived above (Fig. 2B; Eq. 3). Then, the ratio of  $R$  and  $R_A$  measures the cell taper at its apex and reads

$$\frac{R}{R_A} \sim \left( \frac{a}{R_A} \right)^{2/3} \sim \left( \frac{a}{R} \right)^2. \quad (3)$$

This scaling law relates two purely geometrical quantities, the cell radius  $R$  and the apical radius of curvature  $R_A$ , to the size of the secretion region  $a$ , which is essentially controlled by intracellular processes. Given its minimal origins, these laws are expected to hold for a wide range of tip-growing organisms, independent of their particular differences in the molecular and/or cellular mechanisms of cellular morphogenesis.

**Geometrical scaling across species**—Tip-growing cells from different species display different cellular morphologies in the apical growing region (Fig. 1). The scaling relation (Eq. 3) suggests that a quantitative analysis of morphological variation (both intra- and interspecific variation) can help us understand what physical parameters are involved in the control of cellular morphogenesis and provide insights into some of the mechanisms of cellular morphogenesis across species.

To test this, we measured the relation between the apical radius of curvature  $R_A$  and the cell radius  $R$ . Figure 3 shows how the cell radius  $R$  varies with the apical radius of curvature

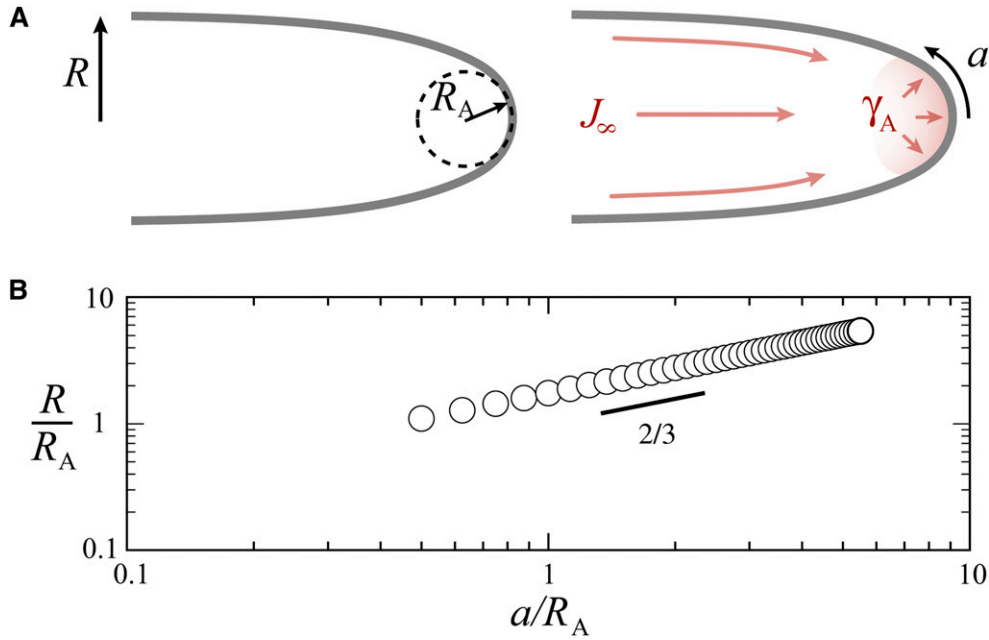


Fig. 2. System definitions and numerically obtained geometrical scaling law. (A) Definition of cell radius  $R$ , apical radius of curvature  $R_A$ , as well as the size  $a$  of the secretion region, the total net flux of new cell wall material transported toward the cell apex  $J_\infty$ , and the apical secretion rate of new cell wall material  $\gamma_A$ . (B) Numerical solutions for  $R/R_A$  as a function of  $a/R$ , obtained from numerical integration of the equations describing cell wall expansion and growth derived in Campas and Mahadevan (2009). The numerical solutions confirm the geometrical scaling law derived in the main text at scaling level (Eq. 3).

$R_A$  for tip-growing cells of varying phylogenetic relatedness (Fig. 1; see Materials and Methods). In all cases, the observed pattern of morphological variation, shows a simple power-law relation between  $R_A$  and  $R$ , consistent with the scaling law derived above (Eq. 3).

Pollen tubes of different angiosperm plant species, as well as hyphae of different fungal species (including the model fungus *Neurospora crassa*), display a scaling behavior where  $R_A \sim R$  (Fig. 3A). Given the previously derived scaling law (Eq. 3), this implies that the size  $a$  of the region over which new cell wall

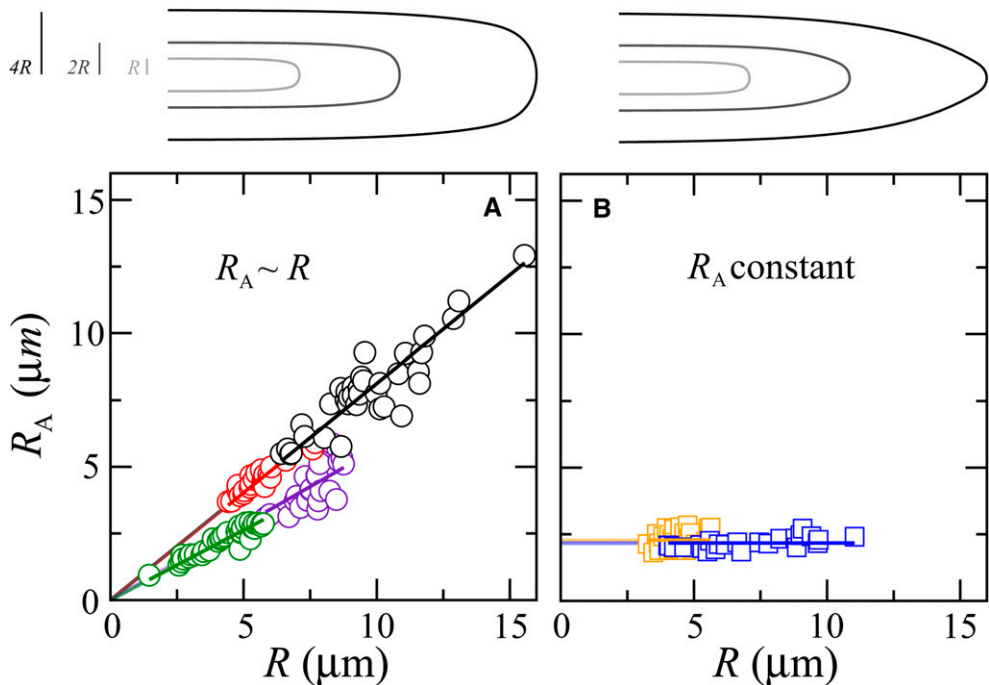


Fig. 3. Measured geometric scaling relations for tip-growing cells in various species. Apical radius  $R_A$  vs. the cell radius  $R$  for several species spanning three major eukaryotic groups (Fig. 1). Color code represents the different species shown in Fig. 1. Pollen tubes of plant species and hyphae from fungal species follow the scaling  $R_A \sim R$  ( $\circ$ ), whereas oomycetes are characterized by a constant apical radius  $R_A$  ( $\square$ ).

material is secreted apically scales with cell size, i.e.,  $a \sim R$ , as does the apical secretion rate  $\gamma_A$ . In this case, the steady shape of the cell is scale invariant, meaning that small and large cells have identical shapes. Furthermore, we see that the slope  $R_A/R$  for pollen tubes of different plant species is very similar (Fig. 3A), and the same result holds for different fungal species. However, plant pollen tubes and fungal hyphae clearly differ in slope  $R/R_A$ , suggesting that more closely related species are characterized by similar slopes.

In contrast, oomycetes (water molds) display a constant apical radius  $R_A$  (Fig. 1B), independent of the cell size  $R$ , consistent with the observation that bigger cells are more pointed. Since  $P$ ,  $\mu_A$ , and  $\rho_w$  are intrinsic quantities, not explicitly dependent on cell geometry, size, or growth rate, the expression  $R_A \sim \mu_A \gamma_A / P \rho_w$  derived earlier indicates that for these species, the apical secretion rate  $\gamma_A$  is constant, independent of cell size. In this case, size  $a$  of the secretion region depends on cell size  $R$  as  $\propto \sqrt[3]{R/R_A}$ . Unfortunately, it has not yet been possible to access the secretion processes directly and measure the size of the secretion region  $a$ , and this is clearly a critical next step to allow a direct test of our predictions.

## DISCUSSION

Our analysis of the role of cell wall assembly and expansion in establishing the shape of tip-growing cells leads to a scaling law (Eq. 3) relating the radius of the cell, the radius of curvature of the apical region, and size of the region where new cell wall material is secreted intracellularly. This relation connects the geometry of the cell to the main intracellular processes involved in the control of cell shape.

We show that the observed morphological variation in tip-growing cells of plant, fungal, and oomycete species are all consistent with this scaling law. Furthermore, we suggest that different strategies in the secretion of new cell wall material lead to different morphologies of tip-growing cells and different patterns of morphological variation. In particular, plant and fungal species seem to control the relative apical secretion rate and size of the secretion region, leading to a scale invariant morphology of the cell, whereas oomycete species seem to maintain a constant apical secretion rate, leading to pointed or oblate cells depending on cell size.

Plant pollen tubes and fungal hyphae display several differences in their respective molecular and cellular mechanisms of morphogenesis (Geitmann and Emons, 2000; Heath and Geitmann, 2000). Our analysis suggests that, despite these differences at the molecular and cellular level, their secretion processes share the same dependence with cell size ( $a \sim R$ ), leading to the same pattern of morphological variation. Therefore, distant species may converge onto the same pattern of morphological variation because of the constraints imposed by mass and force balance.

Moving beyond morphological variation, our scaling law (Eq. 3) also provides a quantitative way to relate cell geometry and intracellular processes, by relating apical geometry to the size of the secretion region. This points to the importance of measuring the size over which new cell wall material is secreted apically in different species with distinct apical geometries. This measure may be obtained via a direct measurement of secretion processes, or indirectly, by measuring the spatial variation in the density of cell wall cross-links away from the growing region. Indeed, the length scale of variation in the density of

cell wall cross-links and the size of the secretion region are very likely coupled. Therefore, a quantitative measure of the spatial variation in cell wall cross-links in tip-growing cells of different species with different apical cell geometries would provide an additional way to test our theoretical predictions.

Since our scaling laws also relate cell radius and apical radius of curvature to the apical secretion rate, the turgor pressure and the apical cell wall viscosity (Eqs. 1, 2; see also Campas and Mahadevan [2009]), experimental control and manipulation of these physical parameters suggest further stringent tests of our theory. For example, the apical secretion rate can be modified by perturbing the transport machinery in the cell, like the motor proteins and cytoskeletal filaments (and several other proteins that regulate these processes) associated to the transport of secretory vesicles. In addition, turgor can be changed by varying the osmolarity of the growth medium. Finally, since the mechanical properties (e.g., its apical viscosity) of a polymeric cell wall depend directly on the degree of cross-linking, one might manipulate this parameter using enzymes with the ability to modify the cross-linking state of the cell wall.

Our framework provides the first steps toward the quantitative relations linking molecular perturbations and morphological phenotypes, so that we may gradually begin to see how intracellular processes affect physical parameters and hence cell shape. Further work is required to reveal whether tip-growing cells extending steadily display only the two patterns of morphological variation reported here (one for plants and fungi and a different one for water molds), or there are many more, with different secretion profiles in space and time to generate shape variation; nevertheless, the cases reported here corresponding to invariant tips and invariant shapes bound the possible morphospaces in tubular, tip-growing cells.

## LITERATURE CITED

- BEADLE, G. W. 1945. Genetics and metabolism in *Neurospora*. *Physiological Reviews* 25: 643–663.
- BOLDUC, J.-F., L. J. LEWIS, C.-E. AUBIN, AND A. GEITMANN. 2006. Finite-element analysis of geometrical factors in micro-indentation of pollen tubes. *Biomechanics and Modeling in Mechanobiology* 5: 227–236.
- BOSCH, M., AND P. K. HEPLER. 2005. Pectin methylesterases and pectin dynamics in pollen tubes. *Plant Cell* 17: 3219–3226.
- CABEEN, M. T., AND C. JACOBS-WAGNER. 2005. Bacterial cell shape. *Nature Reviews Microbiology* 3: 601–610.
- CAMPAS, O., AND L. MAHADEVAN. 2009. Shape and dynamics of tip-growing cells. *Current Biology* 19: 2102–2107.
- CASTLE, E. S. 1958. The topography of tip growth in a plant cell. *Journal of General Physiology* 41: 913–926.
- COLE, R. A., AND J. E. FOWLER. 2006. Polarized growth: Maintaining focus on the tip. *Current Opinion in Plant Biology* 9: 579–588.
- DUMAIS, J., S. L. SHAW, C. R. STEELE, S. R. LONG, AND P. M. RAY. 2006. An anisotropic-viscoplastic model of plant cell morphogenesis by tip growth. *International Journal of Developmental Biology* 50: 209–222.
- FARHADIFAR, R., J.-C. RÖPER, B. AIGOUY, S. EATON, AND F. JÜLICHER. 2007. The influence of cell mechanics, cell–cell interactions, and proliferation on epithelial packing. *Current Biology* 17: 2095–2104.
- FAYANT, P., O. GIRLANDA, Y. CHEBLI, C.-E. AUBIN, I. VILLEMURE, AND A. GEITMANN. 2010. Finite element model of polar growth in pollen tubes. *Plant Cell* 22: 2579–2593.
- GEITMANN, A., AND A. M. EMONS. 2000. The cytoskeleton in plant and fungal cell tip growth. *Journal of Microscopy* 198: 218–245.

- GEITMANN, A., AND J. K. E. ORTEGA. 2009. Mechanics and modeling of plant cell growth. *Trends in Plant Science* 14: 467–478.
- GIERZ, G., AND S. BARTNICKI-GARCIA. 2001. A three-dimensional model of fungal morphogenesis based on the vesicle supply center concept. *Journal of Theoretical Biology* 208: 151–164.
- GILBERT, S. F. 2006. *Developmental biology*, 8th ed. Sinauer, Sunderland, Massachusetts, USA.
- GRIELY, A., AND M. TABOR. 2003. Self-similar tip growth in filamentary organisms. *Physical Review Letters* 90: 108101.
- GREEN, P., R. ERICKSON, AND P. RICHMOND. 1970. On the physical basis for cellular morphogenesis. *Annals of the New York Academy of Sciences* 175: 712–731.
- HAROLD, F. M. 2005. Molecules into cells: Specifying spatial architecture. *Microbiology and Molecular Biology Reviews* 69: 544–564.
- HEATH, I. B., AND A. GEITMANN. 2000. Cell biology of plant and fungal tip growth—Getting to the point. In *The plant cell*, 1513–1517. York University, Biology Department, Toronto, Ontario, Canada.
- HEJNOWICZ, Z., B. HEINEMANN, AND A. SIEVERS. 1977. Tip growth patterns of growth-rate and stress in *Chara* rhizoid. *Zeitschrift für Pflanzenphysiologie* 81: 409–424.
- HEPLER, P. K., L. VIDALI, AND A. Y. CHEUNG. 2001. Polarized cell growth in higher plants. *Annual Review of Cell and Developmental Biology* 17: 159–187.
- HOLDAWAY-CLARKE, T. L., J. A. FEJO, G. R. HACKETT, J. G. KUNKEL, AND P. K. HEPLER. 1997. Pollen tube growth and the intracellular cytosolic calcium gradient oscillate in phase while extracellular calcium influx is delayed. *Plant Cell* 9: 1999–2010.
- KRICHEVSKY, A., S. V. KOZLOVSKY, G.-W. TIAN, M.-H. CHEN, A. ZALTSMAN, AND V. CITOVSKY. 2007. How pollen tubes grow. *Developmental Biology* 303: 405–420.
- KROEGER, J., A. GEITMANN, AND M. GRANT. 2008. Model for calcium dependent oscillatory growth in pollen tubes. *Journal of Theoretical Biology* 253: 363–374.
- LECUIT, T., AND P.-F. LENNE. 2007. Cell surface mechanics and the control of cell shape, tissue patterns and morphogenesis. *Nature Reviews Molecular Cell Biology* 8: 633–644.
- LEW, R. R. 2011. How does a hypha grow? The biophysics of pressurized growth in fungi. *Nature Reviews Microbiology* 9: 509–518.
- LOCKHART, J. A. 1965. An analysis of irreversible plant cell elongation. *Journal of Theoretical Biology* 8: 264–275.
- MACARA, I. G. 2004. Parsing the polarity code. *Nature Reviews Molecular Cell Biology* 5: 220–231.
- MATHUR, J. 2004. Cell shape development in plants. *Trends in Plant Science* 9: 583–590.
- MONEY, N., AND F. HAROLD. 1992. Extension growth of the water mold *Achlya*: Interplay of turgor and wall strength. *Proceedings of the National Academy of Sciences, USA* 89: 4245–4249.
- ORTEGA, J. 1990. Governing equations for plant cell growth. *Physiologia Plantarum* 79: 116–121.
- PELCE, P., AND A. POCHEAU. 1992. Geometrical approach to the morphogenesis of unicellular algae. *Journal of Theoretical Biology* 156: 197–214.
- ROJAS, E. R., S. HOTTON, AND J. DUMAIS. 2011. Chemically mediated mechanical expansion of the pollen tube cell wall. *Biophysical Journal* 101: 1844–1853.
- SCHOPFER, P. 2006. Biomechanics of plant growth. *American Journal of Botany* 93: 1415–1425.
- SHAW, S. L., J. DUMAIS, AND S. R. LONG. 2000. Cell surface expansion in polarly growing root hairs of *Medicago truncatula*. *Plant Physiology* 124: 959–970.
- SIMPSON, A. G. B., AND A. J. ROGER. 2004. The real ‘kingdoms’ of eukaryotes. *Current Biology* 14: R693–R696.
- STEINBERG, G. 2007. Hyphal growth: A tale of motors, lipids, and the Spitzenkörper. *Eukaryotic Cell* 6: 351–360.
- TINDEMANS, S. H., N. KERN, AND B. M. MULDER. 2006. The diffusive vesicle supply center model for tip growth in fungal hyphae. *Journal of Theoretical Biology* 238: 937–948.
- VEYTSMAN, B. A., AND D. J. COSGROVE. 1998. A model of cell wall expansion based on thermodynamics of polymer networks. *Biophysical Journal* 75: 2240–2250.
- VON DASSOW, M., G. M. ODELL, AND D. F. MANDOLI. 2001. Relationships between growth, morphology and wall stress in the stalk of *Acetabularia acetabulum*. *Planta* 213: 659–666.
- WEI, C., AND P. M. LINTILHAC. 2003. Loss of stability—A new model for stress relaxation in plant cell walls. *Journal of Theoretical Biology* 224: 305–312.
- WESTERGAARD, M., AND H. MITCHELL. 1947. *Neurospora* V. A synthetic medium favoring sexual reproduction. *American Journal of Botany* 34: 573–577.
- YOUNG, K. D. 2006. The selective value of bacterial shape. *Microbiology and Molecular Biology Reviews* 70: 660–703.
- ZERZOUR, R., J. KROEGER, AND A. GEITMANN. 2009. Polar growth in pollen tubes is associated with spatially confined dynamic changes in cell mechanical properties. *Developmental Biology* 334: 437–446.